IEEE Access
Multidisciplinary | Rapid Review | Open Access Journal

Received April 21, 2019, accepted May 10, 2019, date of publication May 22, 2019, date of current version June 20, 2019.

Digital Object Identifier 10.1109/ACCESS.2019.2918359

A Dynamic Equivalent Model for DFIG-Based Wind Farms

MINGYANG LIU[1], (Student Member, IEEE), WENXIA PAN[1,2], YIBO ZHANG[3], KUN ZHAO[1], SHIDA ZHANG[3], AND TONGCHUI LIU[1,4]

[1]College of Energy and Electrical Engineering, Hohai University, Nanjing 210098, China
[2]Research Center for Renewable Energy Generation Engineering, Ministry of Education, Hohai University, Nanjing 210098, China
[3]State Grid Henan Electric Power Corporation Maintenance Company, Zhengzhou 450000, China
[4]State Grid Ningbo Power Supply Company, Ningbo 315200, China

Corresponding author: Wenxia Pan (pwxhh@hhu.edu.cn)

This work was supported in part by the National Natural Science Foundation of China under Grant 51377047, in part by the 111 Project of Renewable Energy and Smart Grid under Grant B14022, in part by the Postgraduate Research and Practice Innovation Program of Jiangsu Province under Grant KYCX18_0544, and in part by the Fundamental Research Funds for the Central Universities of China under Grant 2018B674X14.

ABSTRACT With the increasing scale of wind farms, the fault characteristics tend to be complex, which poses a technical challenge to establish the dynamic equivalent model of wind farms. In this paper, a dynamic equivalent method of DFIG-based wind farm based on the density peak clustering algorithm (DPCA) is presented. First, under an analysis of short-circuit current (SCC) in single doubly fed induction generator (DFIG), the clustering indexes are selected. Second, with the selected clustering indexes and DPCA, a more refined two-stage clustering of DFIGs in wind farm is carried out. Third, the units in the same cluster are equivalent to one unit, and then the dynamic equivalent model of the DFIG-based wind farm is established. Finally, the proposed method is validated through the MATLAB/SIMULINK-based simulation results, and the comparison results also show that the dynamic equivalent model proposed in this paper has a better performance than two other equivalent models. Moreover, another comparison between DPCA and K-means clustering algorithm is analyzed, and the result shows that DPCA has a better performance which provides a better choice for dynamic equivalence of wind farms.

INDEX TERMS DFIG-based wind farm, short-circuit current (SCC), dynamic equivalent, density peak clustering algorithm (DPCA).

I. INTRODUCTION

With the increase of wind power penetration in power system, the operation flexibility and security stability of power system have been greatly affected and impacted, so the requirement of analysis and calculation of large-scale wind power connected to the power system is becoming higher [1], [2]. However, when large-scale interconnected system simulation is used to analyze the problems, detailed modeling of each small-capacity wind turbine, transformer and multi-section relatively short collector lines in large-scale wind farms will result in difficult simulation or long simulation time [3], [4]. In order to make the simulation of large-scale interconnected systems run smoothly, a suitable dynamic equivalent model of a wind farm is indispensable [5], [6].

Doubly-fed induction generator (DFIG) has been widely used in wind farms because of its relatively lower cost and better performance [7], [8]. The research object in this paper is the DFIG-based wind farm. The dynamic equivalence of wind farm is based on the fact that the output active power, reactive power and voltage dynamic response at point of common coupling (PCC) of the wind farm are consistent before and after the equivalence [9], [10]. According to mean wind speeds and positive/negative semi-variances of wind speeds, incoming winds are classified in [11], and a group of turbines with similar incoming winds are aggregated together. By calibrating the post-fault power recovery behaviors, an improved single-machine equivalent method for wind farms is proposed in [12]. The clustering method based on the growing spanning tree is applied to the dynamic equivalent of wind farms, and then a simplified dynamic equivalent model of wind farms is proposed in [13]. A geometric template matching based time series wind turbines clustering method is developed in [14]. The Crowbar action conditions (Crowbar action or Crowbar non-action) during the low voltage ride

The associate editor coordinating the review of this manuscript and approving it for publication was Siqi Bu.

through (LVRT) of DFIG are used as the clustering indexes selection in [15]–[17], and the DFIG-based wind farm is described by two equivalent units finally (two-machine equivalent model). However, the above single-machine model and two-machine model are sometimes slightly rough.

Clustering methods and selection of clustering indexes are the important influence factor to the dynamic equivalence of wind farm. K-means clustering algorithm is widely used in computer data mining, distributed energy clustering and other fields because of its fast, simple and high efficiency for large data sets [18]–[21]. The units are divided into groups by using the K-means clustering algorithm, and the units belonging to the same group are considered equivalent to one turbine to realize dynamic equivalent modeling of wind farms [22]. K-means is also used to analyze the clusters to segment the wake effect levels in the wind farms, which results can be used for wake effect levels segmentation in wind farms [23]. With an analysis of the steady-state equation and the third-order transient equation of DFIG, the initial values of 13 state variables are selected as the clustering indexes selection in [24], and the K-means clustering algorithm is used to cluster the units. However, the K-means clustering algorithm is random, so its equivalent effect is sometimes unsatisfactory. Voltage dynamic trajectory of the PCC under a short-circuit fault is presented in [25], [26], to reflect the different degrees of influence of wind turbines. And the index describing the similarity of voltage dynamic trajectory is also defined as the clustering indexes selection of the DFIG-based wind farm. That the transient characteristic differences of DFIGs in a wind farm can be reflected by the SCC of DFIGs when short-circuit faults occur in power grids, is proposed in [27], [28]. And then from the point of the SCC in DFIG, the characteristics describing the similarity of the SCC paths between units is defined and used as a clustering characteristic of wind farms. Therefore, the density peak clustering algorithm (DPCA) and clustering indexes selected from the analysis of SCC of DFIG are applied to the field of wind farm equivalent modeling in this paper.

Based on the analysis of SCC of DFIG, clustering indexes are analyzed and selected. With considering the Crowbar action conditions, and using the selected clustering indexes and DPCA, a more refined two-stage clustering of DFIGs in wind farm is carried out. Then with the units in the same cluster are equivalent to one unit, a dynamic equivalent method of DFIG-based wind farm is given in this paper. This dynamic equivalent method can simplify the wind farm model in large-scale interconnected system simulation under the premise of ensuring accuracy.

II. SYMMETRICAL SHORT-CIRCUIT CURRENT ANALYSIS OF DFIG

A. MATHEMATICAL MODEL OF DFIG

Assuming that the magnetic circuit of the generator is unsaturated, the current and voltage of the stator and rotor windings are prescribed in the normal direction of the motor, and all the electrical quantities of the rotor windings have been converted to the stator winding side. The electromagnetic transient (EMT) equations of DFIG in a synchronously rotating reference frame are given by

$$\begin{cases} \boldsymbol{u}_\mathrm{s} = R_\mathrm{s}\boldsymbol{i}_\mathrm{s} + \mathrm{j}\omega_\mathrm{s}\boldsymbol{\psi}_\mathrm{s} + \dfrac{\mathrm{d}\boldsymbol{\psi}_\mathrm{s}}{\mathrm{d}t} \\ \boldsymbol{u}_\mathrm{r} = R_\mathrm{r}\boldsymbol{i}_\mathrm{r} + \mathrm{j}\omega\boldsymbol{\psi}_\mathrm{r} + \dfrac{\mathrm{d}\boldsymbol{\psi}_\mathrm{r}}{\mathrm{d}t} \\ \boldsymbol{\psi}_\mathrm{s} = L_\mathrm{s}\boldsymbol{i}_\mathrm{s} + L_\mathrm{m}\boldsymbol{i}_\mathrm{r} \\ \boldsymbol{\psi}_\mathrm{r} = L_\mathrm{m}\boldsymbol{i}_\mathrm{s} + L_\mathrm{r}\boldsymbol{i}_\mathrm{r} \end{cases} \tag{1}$$

where $\boldsymbol{u}, \boldsymbol{i}, R, L, \psi$ are the voltage and current, resistance, inductance, and flux, respectively; and the subscripts s and r represent the stator winding and rotor winding, respectively. $L_s = L_{s\sigma} - L_m$ and $L_r = L_{r\sigma} - L_m$, $L_{s\sigma}$ and $L_{r\sigma}$ are the stator leakage inductance and rotor leakage inductance, respectively. L_m is the magnetizing inductance, ω is the slip angular velocity, and ω_s is the synchronous speed.

Then, according to the relationship between flux and current in (1), the SCC of stator and rotor can be expressed as

$$\begin{cases} \boldsymbol{i}_\mathrm{s} = \frac{1}{L_\mathrm{s}'}\boldsymbol{\psi}_\mathrm{s} - k_\mathrm{r}\frac{1}{L_\mathrm{s}'}\boldsymbol{\psi}_\mathrm{r} \\ \boldsymbol{i}_\mathrm{r} = -k_\mathrm{s}\frac{1}{L_\mathrm{r}'}\boldsymbol{\psi}_\mathrm{s} + \frac{1}{L_\mathrm{r}'}\boldsymbol{\psi}_\mathrm{r} \end{cases} \tag{2}$$

where L_s' and L_r' represent the transient inductance of stator winding and rotor winding, respectively. $L_s' = L_{s\sigma} + L_{r\sigma}L_m/(L_{r\sigma} + L_m)$, and $L_r' = L_{r\sigma} + L_{s\sigma}L_m/(L_{s\sigma} + L_m)$. k_s and $k_r$denote the inductance coupling coefficient of stator and rotor, respectively. $k_s = L_m/L_s$, and $k_r = L_m/L_r$.

B. TRANSIENT EQUIVALENT CIRCUIT OF DFIG

Adding Crowbar protection to the rotor winding side is one of the most common and effective methods in the existing LVRT technology for DFIG [29]. Crowbar protection is put into operation when the rotor overcurrent caused by power grid short-circuit fault exceeds the rated capacity of the converter by two times. At the same time, the rotor side converter (RSC) is blocked and the impact large current in the rotor winding is rapidly consumed and attenuated because of the Crowbar resistance. So that the RSC and the grid side converter (GSC) are protected from flowing impact current. Thus, a transient equivalent circuit is established, which is shown in Figure 1.

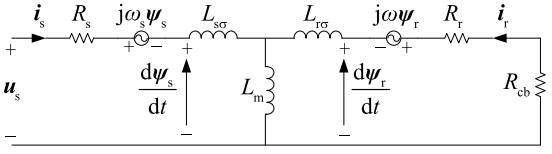

FIGURE 1. The equivalent circuit of a DFIG with the Crowbar resistance.

And meanwhile, the converter is still in a working state when the short-circuit fault of the power grid is insufficient to put Crowbar protection into operation. At this time, another transient equivalent circuit can be also established, which is shown in Figure 2.

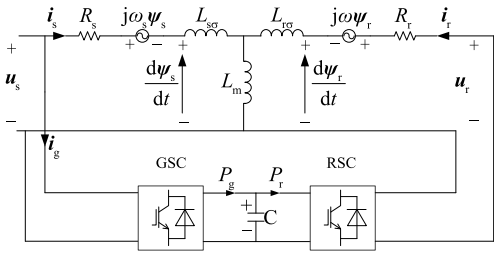

FIGURE 2. The equivalent circuit of a DFIG without the crowbar resistance.

C. ANALYSIS OF SCC FOR DFIG WITH CROWBAR PROTECTION CONNECTED

Assuming the symmetrical short circuit occurs at $t = t_0$, and ignoring the phase jump and transient process of voltage, the voltage before and after the fault can be expressed as

$$\boldsymbol{u}_{\mathrm{s}} = \begin{cases} \boldsymbol{u}_{\mathrm{s0}} = \mathrm{U}_{\mathrm{s0}}\, \mathrm{e}^{\mathrm{j}\alpha}, & t < t_0 \\ \boldsymbol{u}_{\mathrm{sf}} = k\mathrm{U}_{\mathrm{s0}}\, \mathrm{e}^{\mathrm{j}\alpha}, & t \geq t_0 \end{cases} \tag{3}$$

where U_{s0} and U_{sf} are the voltage amplitudes of stator side before and after symmetrical short-circuit occurs, respectively; $\boldsymbol{u}_{\mathrm{s0}}$ and $\boldsymbol{u}_{\mathrm{sf}}$ present the voltage of the stator side in space vector before and after symmetrical short-circuit occurs, respectively; k is the voltage drop factor of stator side, $k = \mathrm{U}_{\mathrm{sf}}/\mathrm{U}_{\mathrm{s0}}$; α is the angle between $\boldsymbol{u}_{\mathrm{s}}$ and d-axis.

Then variation rule of stator flux linkage can be expressed as

$$\boldsymbol{\psi}_{\mathrm{s}} = \begin{cases} \dfrac{\boldsymbol{u}_{\mathrm{s0}}}{\mathrm{j}\omega_{\mathrm{s}}}, & t < t_0 \\ \dfrac{k\boldsymbol{u}_{\mathrm{s0}}}{\mathrm{j}\omega_{\mathrm{s}}} + \dfrac{(1-k)\boldsymbol{u}_{\mathrm{s0}}}{\mathrm{j}\omega_{\mathrm{s}}} \mathrm{e}^{-\mathrm{j}\omega_{\mathrm{s}}(t-t_0)} \mathrm{e}^{-\frac{1}{\tau_{\mathrm{s}}}(t-t_0)}, & t \geq t_0 \end{cases} \tag{4}$$

where τ_{s}' represents the transient time constant of stator, $\tau_{\mathrm{s}}' = L_s'/R_s$.

According to Figure 1 and the relationship between the rotor current and the flux in Equation (2), the voltage equation of the rotor circuit is given by Equation (5).

$$\frac{\mathrm{d}\boldsymbol{\psi}_{\mathrm{r}}}{\mathrm{d}t} + (\mathrm{j}\omega + \frac{1}{\tau_{\mathrm{r}}'})\boldsymbol{\psi}_{\mathrm{r}} = \frac{k_{\mathrm{s}}\boldsymbol{\psi}_{\mathrm{s}}}{\tau_{\mathrm{r}}'},\ t \geq t_0 \tag{5}$$

where τ_{r}' represents the transient time constant of the rotor, $\tau_{\mathrm{r}}' = L_r'/R$ and $R = R_{\mathrm{cb}} + R_{\mathrm{r}}$; R_{cb} is the Crowbar resistance.

According to Equations (2), (4) and (5), the space vector expression of stator current is given by

$$\begin{aligned} \boldsymbol{i}_{\mathrm{s}} = {} & \frac{k\boldsymbol{u}_{\mathrm{s0}}}{\mathrm{j}\omega_{\mathrm{s}}L_{\mathrm{s}}'} + \frac{(1-k)\boldsymbol{u}_{\mathrm{s0}}e^{-\mathrm{j}\omega_{\mathrm{s}}(t-t_0)}e^{-\frac{(t-t_0)}{\tau_{\mathrm{s}}'}}}{\mathrm{j}\omega_{\mathrm{s}}L_{\mathrm{s}}'} \\ & - \frac{k_{\mathrm{r}}k_{\mathrm{s}}k\boldsymbol{R}\boldsymbol{u}_{\mathrm{s0}}}{\mathrm{j}\omega_{\mathrm{s}}L_{\mathrm{r}}'L_{\mathrm{s}}'(\mathrm{j}\omega + 1/\tau_{\mathrm{r}}')} \\ & - \frac{k_{\mathrm{r}}k_{\mathrm{s}}(1-k)\boldsymbol{R}\boldsymbol{u}_{\mathrm{s0}}e^{-\mathrm{j}\omega_{\mathrm{s}}(t-t_0)}e^{-\frac{(t-t_0)}{\tau_{\mathrm{s}}'}}}{\mathrm{j}\omega_{\mathrm{s}}L_{\mathrm{r}}'L_{\mathrm{s}}'(-\mathrm{j}\omega_{\mathrm{r}} - 1/\tau_{\mathrm{s}}' + 1/\tau_{\mathrm{r}}')} \\ & - \frac{k_{\mathrm{r}}C_1e^{-\mathrm{j}\omega(t-t_0)}e^{-\frac{(t-t_0)}{\tau_{\mathrm{r}}'}}}{L_{\mathrm{s}}'} \\ = {} & f_1(\boldsymbol{u}_{\mathrm{s0}}, \boldsymbol{u}_{\mathrm{sf}}, \omega_{\mathrm{s}}, \omega_{\mathrm{r}}, L_{\mathrm{s}}, L_{\mathrm{r}}, L_{\mathrm{m}}, \mathrm{R}_{\mathrm{s}}, \mathrm{R}_{\mathrm{r}}, R_{\mathrm{cb}}, P_{\mathrm{s0}}, Q_{\mathrm{s0}}) \end{aligned} \tag{6}$$

where $C_1 = \boldsymbol{\psi}_{\mathrm{r0}} - \frac{k_{\mathrm{s}}k\boldsymbol{R}\boldsymbol{u}_{\mathrm{s0}}}{\mathrm{j}\omega_{\mathrm{s}}L_{\mathrm{r}}'(\mathrm{j}\omega + 1/\tau_{\mathrm{r}}')} - \frac{k_{\mathrm{s}}(1-k)\boldsymbol{R}\boldsymbol{u}_{\mathrm{s0}}}{\mathrm{j}\omega_{\mathrm{s}}L_{\mathrm{r}}'(-\mathrm{j}\omega_{\mathrm{r}} - 1/\tau_{\mathrm{s}}' + 1/\tau_{\mathrm{r}}')}$.

D. ANALYSIS OF SCC FOR DFIG WITHOUT CROWBAR PROTECTION CONNECTED

When the degree of symmetrical short-circuit fault is insufficient to put Crowbar protection into operation, the converters (RSC and GSC) participate in the transient control of DFIG during short-circuit process. The SCCs in DFIG include the current fed from stator winding (i_{s}) and current fed from GSC, which are as shown in Figure 2.

Referring to the stator-rotor flux relation and rotor voltage expression in Equation (1), and considering that the rotor voltage can accurately track the reference value of rotor voltage, then the second-order differential equation of rotor current can be expressed as Equation (7).

$$\frac{\mathrm{d}\boldsymbol{i}_{\mathrm{r}}^2}{\mathrm{d}^2t} + \mu\frac{\mathrm{d}\boldsymbol{i}_{\mathrm{r}}}{\mathrm{d}t} + \lambda\boldsymbol{i}_{\mathrm{r}} = \lambda\boldsymbol{i}_{\mathrm{r,ref}} + \frac{\tau_{\mathrm{sn}}e_2e^{-\tau_{\mathrm{sn}}t}}{L_{\mathrm{r}}'} \tag{7}$$

where $\boldsymbol{i}_{\mathrm{r,ref}}$ is the reference value space vector of rotor current in the d-q reference frame, which could be calculated by P_{s0} and Q_{s0} [30]; P_{s0} and $Q_{\mathrm{s0}}$are the active power and reactive power before symmetrical short-circuit occurs, respectively; e_2 is the DC component of rotor induced induction electromotive force after fault; $\mu = (R_{\mathrm{r}} + k_{\mathrm{p}} + \mathrm{j}\omega L_{\mathrm{r}}')/L_{\mathrm{r}}'$, $\lambda = k_{\mathrm{i}}/L_r$', k_{p} and k_{i} are the proportional coefficients and the integral time constant of PI controller in inner loop of rotor current.

According to the method of solving second-order non-homogeneous linear ordinary differential equation, the rotor current can be estimated by solving equation (7), the expression is given by

$$\begin{aligned} \boldsymbol{i}_{\mathrm{r}} = {} & \boldsymbol{i}_{\mathrm{r,ref}} + \frac{\tau_{\mathrm{sn}}e_2e^{-\tau_{\mathrm{sn}}t}}{L_{\mathrm{r}}'(\tau_{\mathrm{sn}}^2 - \tau_{\mathrm{sn}}\mu + \lambda)} \\ & + \frac{-\alpha_2\boldsymbol{i}_{\mathrm{r0}}e^{\alpha_1(t-t_0)} + \alpha_1\boldsymbol{i}_{\mathrm{r0}}e^{\alpha_2(t-t_0)}}{\alpha_1 - \alpha_2} \end{aligned} \tag{8}$$

where $\boldsymbol{i}_{\mathrm{r0}}$ is the initial value of rotor current; α_1 and α_2 are the characteristic roots of the ordinary differential equation, $\alpha_1 = (-\mu + \sqrt{\mu^2 - 4\lambda})/2$, and $\alpha_2 = (-\mu - \sqrt{\mu^2 - 4\lambda})/2$;

According to the relationship between stator current and stator flux linkage in Equation (2), the SCC component $\boldsymbol{i}_{\mathrm{s}}$ can be expressed by Equation (9).

$$\begin{aligned} \boldsymbol{i}_{\mathrm{s}} = {} & \frac{k\boldsymbol{u}_{\mathrm{s0}}}{\mathrm{j}\omega_{\mathrm{s}}L_{\mathrm{s}}} + \frac{(1-k)\boldsymbol{u}_{\mathrm{s0}}}{\mathrm{j}\omega_{\mathrm{s}}L_{\mathrm{s}}}e^{-\mathrm{j}\omega_{\mathrm{s}}(t-t_0)}e^{-\frac{1}{\tau_{\mathrm{s}}}(t-t_0)} - \frac{L_{\mathrm{m}}}{L_{\mathrm{s}}}\boldsymbol{i}_{\mathrm{r,ref}} \\ & - \frac{L_{\mathrm{m}}}{L_{\mathrm{s}}}\frac{\tau_{\mathrm{sn}}e_2e^{-\tau_{\mathrm{sn}}t}}{L_{\mathrm{r}}'(\tau_{\mathrm{sn}}^2 - \tau_{\mathrm{sn}}\mu + \lambda)} \\ & - \frac{L_{\mathrm{m}}}{L_{\mathrm{s}}}\frac{-\boldsymbol{\alpha}_2\boldsymbol{i}_2i_{10}e^{q_1(t-t_0)} + \boldsymbol{\alpha}_1i_{10}e^{a_1(t-t_0)}}{\boldsymbol{\alpha}_1 - \boldsymbol{\alpha}_2} \end{aligned} \tag{9}$$

The SCC component $\boldsymbol{i}_{\mathrm{g}}$ is smaller than $\boldsymbol{i}_{\mathrm{s}}$. According to the exchange power balance relationship between the GSC and

RSC under the steady state of a short circuit fault, the following relationship is established

$$\boldsymbol{i}_{\mathrm{g}} = s\boldsymbol{i}_{\mathrm{r}} \tag{10}$$

where s is the slip ratio of the generator,$s = (\omega_{\mathrm{s}} - \omega_{\mathrm{r}})/\omega_{\mathrm{s}}$.

According to Equations (8), (9) and (10), the SCC without Crowbar protection can be approximately estimated by Equation (11).

$$\begin{aligned}\boldsymbol{i} &= \boldsymbol{i}_{\mathrm{s}} + \boldsymbol{i}_{\mathrm{g}} \\ &= \frac{k\boldsymbol{u}_{\mathrm{s0}}}{\mathrm{j}\omega_{\mathrm{s}}L_{\mathrm{s}}} + \frac{(1-k)\boldsymbol{u}_{\mathrm{s0}}}{\mathrm{j}\omega_{\mathrm{s}}L_{\mathrm{s}}} e^{-\mathrm{j}\omega_{\mathrm{s}}(t-t_0)} e^{-\frac{1}{\tau_{\mathrm{s}}}(t-t_0)} \\ &\quad - \left(\frac{L_{\mathrm{m}}}{L_{\mathrm{s}}} - s\right)\boldsymbol{i}_{\mathrm{r,ref}} - \left(\frac{L_{\mathrm{m}}}{L_{\mathrm{s}}} - s\right)\frac{\tau_{\mathrm{sn}}e_2 e^{-\tau_{\mathrm{sp}}t}}{L'_{\mathrm{r}}\left(\tau_{\mathrm{sn}}^2 - \tau_{\mathrm{sn}}\mu + \lambda\right)} \\ &\quad - \left(\frac{L_{\mathrm{m}}}{L_{\mathrm{s}}} - s\right)\frac{-\alpha_2\boldsymbol{i}_{\mathrm{r0}}e^{\alpha_1(t-t_0)} + \alpha_1\boldsymbol{i}_{\mathrm{r0}}e^{\alpha_2(t-t_0)}}{\alpha_1 - \alpha_2} \\ &= f_2(\boldsymbol{u}_{\mathrm{s0}}, \boldsymbol{u}_{\mathrm{sf}}, \omega_{\mathrm{s}}, \omega_{\mathrm{r}}, L_{\mathrm{s}}, L_{\mathrm{r}}, L_{\mathrm{m}}, R_{\mathrm{s}}, R_{\mathrm{r}}, k_{\mathrm{p}}, k_{\mathrm{i}}, P_{\mathrm{s0}}, Q_{\mathrm{s0}})\end{aligned} \tag{11}$$

III. A DYNAMIC EQUIVALENT METHOD OF DFIG-BASED WIND FARM

A. CLUSTERING INDEXES SELECTION AND CLUSTERING METHOD OF DFIG-BASED WIND FARM

The SCC of DFIG is a very important index which can reflect the different operation points of DFIGs in wind farm, during the transient process after short-circuit fault of power grid [29], [31]. Therefore, based on the model analysis of DFIG under a symmetrical short-circuit fault, the clustering indexes selection used to the division of the different operation states of the unit are studied in this section.

Equation (6) is used to analyze the factors affecting the symmetrical SCC of DFIG when Crowbar protection connected, and then the clustering indexes are extracted to divided different clusters.

For the same type of DFIG, no matter what kind of working conditions the unit runs, the synchronous speed ω_{s}, stator inductance L_{s}, rotor inductanceL_{r}, mutual inductanceL_{m}, stator resistance R_{s} and rotor resistanceR_{r} are equal and fixed, and the same value of Crowbar resistanceR_{cb}, is used in all the units in this section. Moreover, in this paper, when considering the factors affecting the short-circuit current to extract the clustering indexes selection to divide different clusters, only the physical quantities which change during the calculation of SCC and the different physical quantities between the units are explored. Therefore, according to the analysis of the expression of DFIG symmetrical SCC with Crowbar protection connected, the clustering characteristic parameters used in the cluster division can be extracted as $\boldsymbol{u}_{\mathrm{s0}}$, $\boldsymbol{u}_{\mathrm{sf}}$, ω_{r}, P_{s0}, and Q_{s0}.

Similarly, Equation (11) is used to analyze the factors affecting the symmetrical SCC of DFIG when Crowbar protection is not connected, and then the clustering indexes selected are also extracted to divided different clusters. For the same type DFIG without Crowbar protection connected, ω_{s}, L_{s}, L_{r}, L_{m}, R_{s}, R_{r} and R_{cb} are also the same, and moreover, the proportional and integral coefficients (i.e., k_{p} and k_{i}) of the PI controller in the RSC are equal and fixed. Thus, the clustering indexes selection in this case can be also extracted as $\boldsymbol{u}_{\mathrm{s0}}$, $\boldsymbol{u}_{\mathrm{sf}}$, ω_{r}, P_{s0}, and Q_{s0}.

When a short-circuit fault occurs in the power grid, there are probably two types of DFIG, units with and without Crowbar protection connected, in the large-scale DFIG-based wind farm. Therefore, the judgment of the Crowbar protection state is the first step in clustering in this paper. And due to the different initial operation state of DFIGs, the transient characteristics of each unit under the fault are also different. So secondly, for the units which Crowbar protections are connected, the selected clustering indexes selection and clustering algorithm are used to the further divisions. Thirdly, the same clustering measures are used in units without Crowbar protection connected.

B. CLUSTERING ALGORITHM BASED ON PEAK DENSITY

In this paper, using the selected clustering features, a density peak clustering algorithm (DPCA) is used to cluster the units. The peculiarity of DPCA lies in its characterization of clustering centers. It holds that the clustering center has two characteristics: one is its own large density, that is, it is surrounded by its neighbors whose density is not larger than it; the other is that the "distance" from other denser data points is relatively larger [32]. The definition of DPCA is introduced as below.

For a data set ($\mathrm{S} = \{x_i\}, i \in I = (1, 2, \ldots, N)$) to be clustered, is a set of the clustering indexes ($\boldsymbol{u}_{\mathrm{s0}}$, $\boldsymbol{u}_{\mathrm{sf}}$, ω_{r}, P_{s0}, and Q_{s0}) for each DIFG. Some distance (such as Euclidean distance) between any two data points (x_i and x_j) in the data set is expressed as d_{ij}. Then local density ρ_i and distance δ_i can be defined by any data point x_i of the data set, to describe the characteristics of the clustering center.

The definition of ρ_i is expressed as Equation (12).

$$\rho_i = \sum_{i,j \in I} \chi(d_{ij} - d_c) \tag{12}$$

where $\chi(x) = \begin{cases} 1, x < 0 \\ 0, x > 0 \end{cases}$; d_c is the truncated distance, $d_c > 0$.

The definition of δ_i is expressed as Equation (13).

$$\delta_i = \begin{cases} \min\limits_{j \in I_{\mathrm{s}}} \{d_{ij}\} & I_{\mathrm{s}} \neq \emptyset \\ \max\limits_{j \in I} \{d_{ij}\} & I_{\mathrm{s}} = \emptyset \end{cases} \tag{13}$$

where $I_{\mathrm{s}} = \{k \in I : \rho_k \geq \rho_i\}$.

According to the definition, ρ_i denotes the sum of the number of data points (not considering x_i) whose distance from the x_i in the data set S is less than a certain truncation distance d_{c} (as a rule of thumb, d_{c} is set as 0.05 in this paper); δ_i denotes the minimum value of a certain distance d_{ij} from the data point x_i to another data point in the specific data sets (all data are taken from the data set S), which composed of x_j, whose ρ_j is not less than ρ_i; and when the local density ρ_i of

data points x_i in the data set S is the largest, the distance is obtained, $\delta_i = \max_{j \in I} \{d_{ij}\}$.

Thus, for each data point xi in the data set S, there is a pair of binary data (ρ_i, δ_i) which describes its characteristics. All binary data pairs are represented on the two-dimensional plane with ρ_i as horizontal axis and δ_i as vertical axis. The two-dimensional plane is usually called cluster center decision graph. In order to ensure the number of clustering centers, a new variable is defined in this algorithm.

$$\gamma_i = \rho_i \delta_i \tag{14}$$

According to the description of the characteristics of the clustering center in DPCA, the larger the γ in the data point is, the more likely it is the clustering center. Usually a diagram of the descending order of values is given, which takes values as ordinates and the number of data points as abscissas.

Usually a diagram of the descending order of γ is given, which takes γ as ordinate and the number of data points n_0 as abscissa. The points above the obvious breakpoints in the graph can be chosen as the cluster center [32].

C. JUDGMENT METHOD OF CROWBAR PROTECTION ACTION OF DFIG

When the rotor current of DFIG exceeds two times of its rated value, Crowbar protection action will be performed, otherwise Crowbar protection will not be put into operation. If the rotor current of each unit in a large wind farm is calculated separately, the calculation will be complicated and the workload will be large. Therefore, this paper proposes a simple and intuitive way to judge whether Crowbar protection is connected.

According to the analysis of rotor current before Crowbar protection action (Equation (8)), the criterion of Crowbar protection action can be transformed into the function relation between voltage drop variable ΔU under certain power factor condition, active power P_{s0} and terminal voltage phase Φ. Then through the simulation of the corresponding type of units, the curved surface function for judging whether the Crowbar protection works under the typical power factor is established, which is shown in Figure 3. Here, the curved surface function is expressed simply by $\Delta U = f(P_{s0}, \Phi)$.

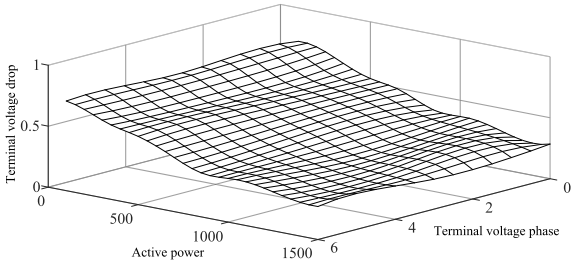

FIGURE 3. The curved surface of crowbar protection operation.

The judging steps are as follows:

Step 1: input the P_{s0} and Φ of a DFIG;

Step 2: estimate the critical operating voltage, $\Delta U_{cr} = f(P_{s0}, \Phi)$;

Step 3: Compare the critical operating voltage, ΔU_{cr}, and the terminal voltage drop, ΔU;

Step 4: if $\Delta U \geq \Delta U_{cr}$, the Crowbar protection of this DFIG will be connected; otherwise, the Crowbar protection will not be put into operation.

D. CALCULATION METHOD OF EQUIVALENT MODEL PARAMETERS

1) CALCULATION OF EQUIVALENT WIND SPEED

In order to calculate the equivalent wind speed, the wind energy utilization coefficient of the equivalent wind turbine can be set by [33].

$$C_{peq} = \frac{1}{m} \sum_{i=1}^{m} C_{pi} \tag{15}$$

where C_{pi} is the wind energy utilization coefficient of wind turbines in the same cluster, m is the number of wind turbines in the same cluster, and the subscript eq means the value under equivalence.

According to the relationship between the mechanical power captured by the wind turbine before and after the equivalence, the input wind speed of the equivalent wind turbine can be estimated by Equation (16).

$$v_{weq} = \left(\frac{\sum_{i=1}^{m} C_{pi} v_{wi}^3}{m C_{peq}}\right)^{\frac{1}{3}} \tag{16}$$

2) PARAMETER CALCULATION OF EQUIVALENT GENERATOR

The units in the same cluster can be equivalent to one unit. Its parameters can be estimated by Equation (17).

$$\begin{cases} S_{eq} = mS, R_{eq} = R/m, L_{eq} = L/m \\ C_{eq} = mC, H_{eq} = H, D_{eq} = D \\ K_{eq} = K, R_{cb_{eq}} = R_{cb}/m \\ S_{T_{eq}} = mS_T, Z_{T_{eq}} = Z_T/m \end{cases} \tag{17}$$

where S is the apparent capacity of the unit; R, L and C are the nominal values of the resistance, reactance and capacitance of the unit, respectively; H, D and K are the inertia time constant, damping coefficient and rigidity coefficient of the unit, respectively; S_T and Z_T are the nominal values of the capacity and impedance of each transformer, respectively.

The calculation of parameters can be applied to wind farm with different topologies and different physical locations, but the same type of DFIGs.

E. EVALUATION OF EQUIVALENCE EFFECT

In order to measure the accuracy of the equivalent methods of different wind farms, the indexes of active power error $E_P(\%)$, reactive power error $E_Q(\%)$ and voltage error $E_U(\%)$ are usually introduced [34], [35]. Generally, the descriptions

of their definitions are given as follows

$$E_P(\%) = \frac{\sum_{i=1}^{n} |P_i - P_{0i}|}{\sum_{i=1}^{n} |P_i|} \times 100 \quad (18)$$

$$E_Q(\%) = \frac{\sum_{i=1}^{n} 2\,|Q_i - Q_{0i}|}{\sum_{i=1}^{n} |S - 2Q_{0i}|} \times 100 \quad (19)$$

$$E_U(\%) = \frac{\sum_{i=1}^{n} |U_i - U_{0i}|}{\sum_{i=1}^{n} |U_i|} \times 100 \quad (20)$$

where i is the i^{th} data point under a certain step in the simulation; P_i, Q_i and U_i are the active power, reactive power and voltage at the PCC point corresponding to the i^{th} data point under an equivalent method, respectively; P_{0i}, Q_{0i} and U_{0i} are the active power, reactive power and voltage at the PCC point corresponding to the i^{th} data point under the detailed model of the wind farm, respectively.

The computational flow of the presented method is as shown in Fig.4.

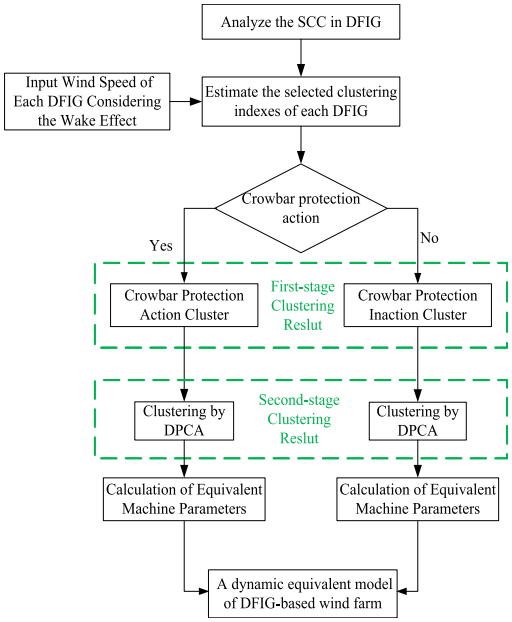

FIGURE 4. The computational flow of the presented method.

IV. SIMULATION AND RESULT ANALYSIS

A wind farm network as Figure 5 shown is built in MATLAB/SIMULINK to verify the proposed dynamic equivalent method for the DFIG-based wind farms. The units are arranged in 5 rows and 5 columns. And the wind farm is under the standard air density, the incoming wind speed is 13m/s and the wind direction is 30°. Other parameters of the

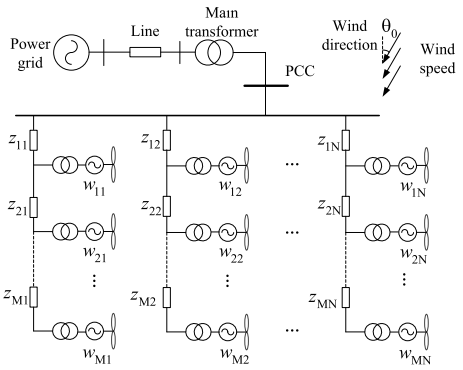

FIGURE 5. Topological structure of wind farm before equivalent.

wind farm are shown in Appendix A. According to the wind speed and direction, and considering the wake effect, the wind speed of each unit in the wind farm can be calculated as shown in Appendix B.

The power factor of DFIG is set as 1, when a symmetrical short-circuit fault occurs at the low-voltage side of the main transformer, the inter-phase transition resistance is 1.7 ohms and the fault duration is 500 ms, the voltage at PCC of the wind farm drops to 63.2%.

Then, according to the wind speed of each DFIG, the active power can be obtained from the wind speed-power curve in the technical manual of this type of DFIG, and the reactive power of each unit can be calculated from the power factor. According to the power flow calculation, the initial voltage of each unit in the wind farm can be obtained as shown in Appendix C. The DFIG unit is equivalent to the sub-transient potential and the sub-transient reactance, and the steady-state voltage values of the wind farm units under the short-circuit fault can be obtained as shown in Appendix D. The rotor speed of each unit in the wind farm can be found by the speed-power curve in the DFIG technical manual of this type. Without considering the effect of voltage phase jump before and after short circuit fault, the phase Φ of each terminal voltage under short-circuit fault can be estimated as follows,

$$\Phi = \Phi_1 + \Delta\Phi \quad (21)$$

where, Φ_1 is the phase value of voltage at the low-voltage side of the main transformer, $\Delta\Phi$ is the difference value between the unit voltage and the low voltage side of the main transformer.

According to the method of judging Crowbar protection state in Section 2.4, the result of judging Crowbar protection action is shown in Table 1. In this table, "$\surd$" presents that the Crowbar protection is connected, "x" presents that the Crowbar protection is not connected.

Using the calculated clustering indexes selection, the further divisions of the units with and without Crowbar protection operation is carried out again. The clustering basis obtained by DPCA is given in Figure 6 and Figure 7.

Obviously, there are 2 cluster centers for 9 units with Crowbar protection operation, which can be grouped into

TABLE 1. Judgment results of crowbar protection operation for different units.

j	1	2	3	4	5
w_{1j}	√	√	√	√	√
w_{2j}	√	x	x	x	√
w_{3j}	x	x	x	x	√
w_{4j}	x	x	x	x	√
w_{5j}	x	x	x	x	x

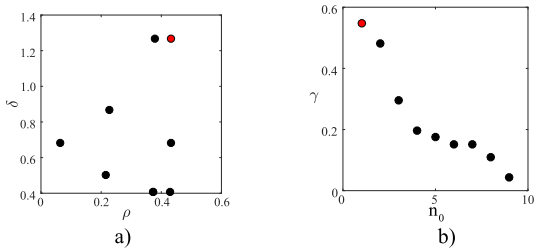

FIGURE 6. Clustering basis of units with Crowbar protection operation. a) Decision diagram of the cluster center. b) Schematic diagram of γ descending order.

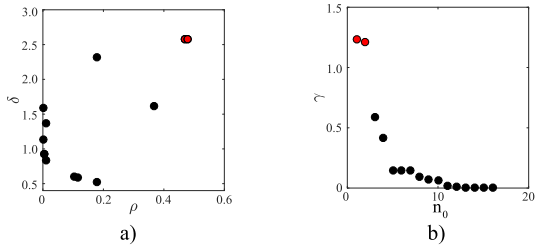

FIGURE 7. Clustering basis of units without Crowbar protection operation. a) Decision diagram of the cluster center. b) Schematic diagram of γ descending order.

TABLE 2. Clustering results of wind farms.

Crowbar protection state	Equivalents	Clustering results
√	1	w_{11}, w_{12}, w_{13}, w_{14}, w_{15}
√	2	w_{21}, w_{25}, w_{35}, w_{45}
x	3	w_{31}, w_{32}, w_{42}, w_{52}
x	4	w_{33}, w_{34}, w_{43}, w_{53}
x	5	w_{22}, w_{23}, w_{24}
x	6	w_{41}, w_{44}, w_{51}, w_{54}, w_{55}

2 clusters, and the final result is 2 equivalent units; for 16 units without Crowbar protection operation, there are 4 cluster centers, which can be grouped into 4 clusters, thus the final result is 4 equivalent units. Table 2 shows the final clustering results of wind farms.

According to the equivalent method of the equivalent wind speed and collector lines, the wind speed of each equivalent unit is 13m/s, 13m/s, 11.1719m/s, 9.3866m/s, 11.1719m/s and 8.1686m/s, respectively. Meanwhile the corresponding collector line length is calculated to be 0.45km, 1.30km, 0.76km, 0.72km, 0.78km and 1.04km, respectively, where the impedance of unit length of collector line has not changed. And the parameters of the equivalent units are estimated using the method introduced insection 3.3.

DFIG-based wind farm models with different equivalent methods, the equivalent method proposed in this paper (PEM), the single-machine equivalent method (SEM) [36], and the two-machine equivalent method (TEM) [15], are built on the MATLAB/SIMULINK platform and simulated. The equivalent effect of different equivalent methods is shown in Figure 8.

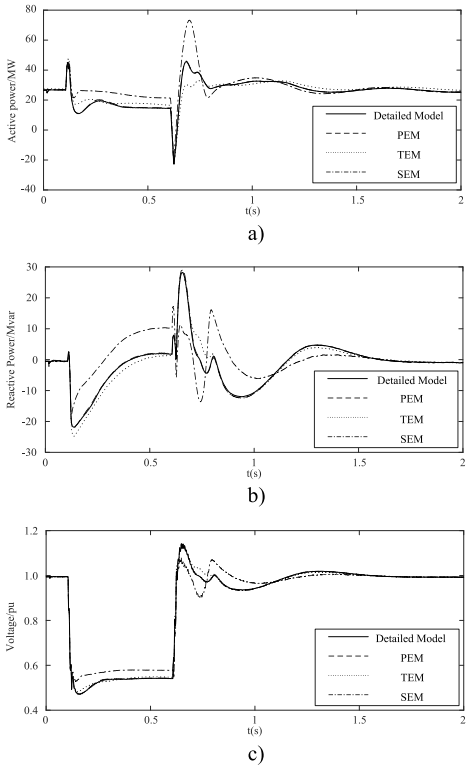

FIGURE 8. Equivalence effect of different equivalent models. a) Active power of PCC in wind farm. b) Reactive power of PCC in wind farm. c) Voltage of PCC in wind farm.

Using the index defined in Section III of this paper to evaluate the dynamic equivalent effect of wind farms, the errors between different equivalent methods and detailed models are compared, and the results are given in Table 3. It can be found from table 3 that the wind farm equivalent model proposed in this paper is closer to the detailed wind farm model than the two-machine equivalent model and the single-machine equivalent model.

The comparison results of the current responses are as shown in Figure 9.

As shown in Figure 9, the proposed model has good results in current responses. Moreover it can accommodate different operational scenarios, and the authors hold a positive view on whether the model can accommodate to asymmetric faults.

TABLE 3. Errors between different equivalent models and detailed models.

Equivalent method	E_P (%)	E_Q (%)	E_U (%)
PEM	0.57	0.82	0.12
TEM	8.25	4.07	0.53
SEM	15.11	20.70	2.71

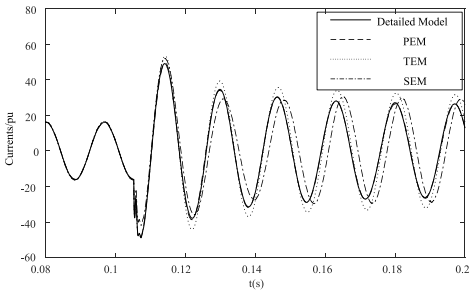

FIGURE 9. Current responses comparison of different equivalent models.

Moreover, the effect comparison between DPCA and K-means clustering algorithm which is widely used in dynamic equivalence of wind farms is analyzed in this paper. There are two ways to select K, which are shown as follows.

"K-means1": based on the number of clusters given by the DPCA method. The units with Crowbar protection operation are divided into two clusters and the units without Crowbar protection operation are divided into four clusters. There are three different clustering results in this method through many attempts.

"K-means2": based on human designation. The units with Crowbar protection operation are divided into one cluster and the units without Crowbar protection operation are divided into three clusters. Similarly, there are five different clustering results in this method through attempts. The detailed clustering results are no longer listed in this paper. Table 4 shows the equivalence effect of different clustering results.

Because the cluster result of the in "K-means1" and the DPCA is the same, it can be seen from table 4 that the error of the is the same as the error of DPCA in table 3. The error of the other two results (and) of "K-means1" is obviously inferior to that of DPCA. Meanwhile, the "K-means 2" method-based equivalent effect is also inferior to the DPCA-based equivalent effect. On the one hand, the effect is influenced by the subjective will; on the other hand, the effect is influenced by the random selection of initial clustering center, which is the inherent defect of K-means clustering algorithm.

V. CONCLUSION

With the increasing scale of wind farms, a suitable dynamic equivalent model of wind farm is indispensable. This paper provides a dynamic equivalent method of DFIG-based wind farms with DPCA and SCC clustering indexes, in which there are three main contributions:

1) Based on the symmetrical SCC analysis of DFIG, the clustering indexes for the dynamic equivalence of DFIG-based wind farms are extracted in this paper. That is the fault-front terminal voltage $\boldsymbol{u}_{s0}$, fault-end terminal voltage $\boldsymbol{u}_{sf}$, rotor speed ω_r, active power P_{s0}, and reactive power Q_{s0}.

2) A more refined two-stage clustering of DFIGs in wind farm is carried out. According to the judgment of Crowbar protection state, the units in wind farms are divided into two clusters firstly; secondly, the selected clustering indexes

TABLE 4. Clustering results and equivalence effects of different clustering algorithms.

Clustering Algorithms	Cluster Results	E_P (%)	E_Q (%)	E_U (%)
DPCA	①	0.57	0.82	0.12
K-means1	①	2.83	1.8	0.25
	②	1.74	4.04	0.42
	③	0.57	0.82	0.12
K-means2	①	1.24	0.85	0.14
	②	0.71	0.77	0.13
	③	3.76	2.34	0.27
	④	3.02	1.78	0.27
	⑤	3.38	2.37	0.36

TABLE 5. Parameters in the wind farm.

Part	Parameters	Value
DFIG	Rated Power	1.5 MW
	Rated Voltage	575 V
	Rs	0.023 p.u.
	Rr	0.016 p.u.
	Lm	2.9 p.u.
	Ls	0.18 p.u.
	Lr	0.16 p.u.
	kp	0.6
	ki	8
Terminal transformer	Rated capacity	1.75 MVA
	Voltage ratio	25 kV /0.575 kV
Main transformer	Rated capacity	47 MVA
	Voltage ratio	25 kV /120 kV
Overhead / collector line	R	0.115 Ω/km
	L	1.05e-3 H/km
Overhead line	Length	30 km
Group row distance	Length	0.5 km
Group column distance	Length	0.25 km

TABLE 6. Wind speed of each unit in the wind farm (m/s).

j	1	2	3	4	5
w_{1j}	13.000 0	13.000 0	13.000 0	13.000 0	13.000 0
w_{2j}	13.000 0	11.171 9	11.171 9	11.171 9	13.000 0
w_{3j}	11.171 9	11.171 9	9.386 6	9.386 6	13.000 0
w_{4j}	9.386 6	11.171 9	9.386 6	7.965 5	13.000 0
w_{5j}	7.965 5	11.171 9	9.386 6	7.965 5	7.154 0

TABLE 7. Initial voltage of each unit in the wind farm (p.u.).

j	1	2	3	4	5
w_{1j}	1.001 0	1.000 7	1.000 2	1.000 5	1.001 2
w_{2j}	1.001 2	1.000 9	1.000 3	1.000 7	1.001 4
w_{3j}	1.001 4	1.001 0	1.000 3	1.000 7	1.001 6
w_{4j}	1.001 4	1.001 2	1.000 5	1.000 7	1.001 6
w_{5j}	1.001 2	1.001 2	1.000 5	1.000 7	1.001 4

TABLE 8. Steady-state voltage of units in the wind farm under the short-circuit fault (p.u.).

j	1	2	3	4	5
w_{1j}	0.634 9	0.633 3	0.631 7	0.633 3	0.634 9
w_{2j}	0.640 1	0.638 5	0.636 9	0.638 5	0.640 1
w_{3j}	0.644 2	0.642 6	0.640 9	0.642 6	0.644 2
w_{4j}	0.646 9	0.645 3	0.643 6	0.645 3	0.646 9
w_{5j}	0.648 3	0.646 7	0.645 0	0.646 7	0.648 3

selection and the clustering method are used to the further divisions; finally, the same cluster is equivalent to one unit, which is the final dynamic equivalent model of DFIG-based wind farms.

3) DPCA is applied to the field of wind farm equivalent modeling as a clustering method in this paper. And with the analysis of the effect comparison between DPCA and K-means clustering algorithm, the DPCA has a better effect.

With the challenges of large-scale interconnected system simulation, an accurate and efficient dynamic equivalent model of wind farms is desired. We believe that the proposed method will serve well in this regard.

APPENDIX

A. PARAMETERS IN THE WIND FARM

See Table 5.

B. WIND SPEED OF EACH UNIT IN THE WIND FARM

See Table 6.

C. THE INITIAL VOLTAGE OF EACH UNIT IN THE WIND FARM

See Table 7.

D. STEADY-STATE VOLTAGE OF UNITS IN THE WIND FARM

See Table 8.

REFERENCES

[1] W. Du, X. Chen, and H. Wang, "Impact of dynamic interactions introduced by the DFIGs on power system electromechanical oscillation modes," *IEEE Trans. Power Syst.*, vol. 32, no. 6, pp. 4954–4967, Nov. 2017.

[2] M. Firouzi, G. B. Gharehpetian, and B. Mozafari, "Power-flow control and short-circuit current limitation of wind farms using unified interphase power controller," *IEEE Trans. Power Del.*, vol. 32, no. 1, pp. 62–71, Feb. 2017.

[3] P. Ju, H. Li, C. Gan, Y. Liu, Y. Yu, and Y. Liu, "Analytical assessment for transient stability under stochastic continuous disturbances," *IEEE Trans. Power Syst.*, vol. 33, no. 4, pp. 2004–2014, Mar. 2018.

[4] W. Li, P. Chao, X. Liang, J. Ma, D. Xu, and X. Jin, "A practical equivalent method for DFIG wind farms," *IEEE Trans. Sustain. Energy*, vol. 9, no. 2, pp. 610–620, Apr. 2017.

[5] F. Liu, J. Ma, W. Zhang, and M. Wu, "A comprehensive survey of accurate and efficient aggregation modeling for high penetration of large-scale wind farms in smart grid," *Applid Sci.-Basel*, vol. 9, no. 4, p. 769, Feb. 2019.

[6] J. Zou, C. Peng, Y. Yan, H. Zheng, and Y. Li, "A survey of dynamic equivalent modeling for wind farm," *Renew. Sustain. Energy Rev.*, vol. 40, pp. 956–963, Dec. 2014.

[7] D. Howard, J. Liang, and R. Harley, "Short-circuit modeling of DFIGs with uninterrupted control," *IEEE J. Emerg. Sel. Topics Power Electron.*, vol. 2, no. 1, pp. 47–57, Mar. 2014.

[8] M. Liu, W. Pan, R. Quan, H. Li, T. Liu, and G. Yang, "A short-circuit calculation method for DFIG-based wind farms," *IEEE Access*, vol. 6, pp. 52793–52800, 2018.

[9] J. Zou, C. Peng, H. Xu, and Y. Yan, "A fuzzy clustering algorithm-based dynamic equivalent modeling method for wind farm with DFIG," *IEEE Trans. Energy Convers.*, vol. 30, no. 4, pp. 1329–1337, Dec. 2015.

[10] H. Zhou, P. Ju, Y. Xue, and J. Zhu, "Probabilistic equivalent model of DFIG-based wind farms and its application in stability analysis," *J. Mod. Power Syst. Clean Energy*, vol. 4, no. 2, pp. 225–248, 2016.

[11] Z. Meng, F. Xue, and X. Li, "Wind speed equalization-based incoming wind classification by aggregating DFIGs," *J. Mod. Power Syst. Clean Energy*, vol. 1, no. 1, pp. 42–48, Jun. 2013.

[12] W. Li, P. Chao, X. Liang, D. Xu, and X. Jin, "An improved single-machine equivalent method of wind power plants by calibrating power recovery behaviors," *IEEE Trans. Power Syst.*, vol. 33, no. 4, pp. 4371–4381, Jul. 2018.

[13] W. Teng, X. Wang, Y. Meng, and W. Shi, "Dynamic clustering equivalent model of wind turbines based on spanning tree," *J. Renew. Sustain. Energy*, vol. 7, no. 6, 2015, Art. no. 063126.

[14] P. Wang, Z. Zhang, Q. Huang, N. Wang, X. Zhang, and W.-J. Lee, "Improved wind farm aggregated modeling method for large-scale power system stability studies," *IEEE Trans. Power Syst.*, vol. 33, no. 6, pp. 6332–6342, Nov. 2018.

[15] Y. H. Yan and W. Feng, "Short-circuit current analysis for DFIG wind farm considering the action of a crowbar," *Energies*, vol. 11, no. 2, p. 425, Feb. 2018.

[16] Y. Gao, Y. Jin, P. Ju, and Q. Zhou, "Dynamic equivalence of wind farm composed of double fed induction generators considering operation characteristic of crowbar," *Power Syst. Technol.*, vol. 39, pp. 628–633, Mar. 2015.

[17] Q. Zhu, M. Ding, and P. Han, "Equivalent modeling of DFIG-based wind power plant considering crowbar protection," *Math. Problems Eng.*, vol. 2016, Jun. 2016, Art. no. 8426492.

[18] R. Achanta, A. Shaji, K. Smith, A. Lucchi, P. Fua, and S. Süsstrunk, "SLIC superpixels compared to state-of-the-art superpixel methods," *IEEE Trans. Pattern Anal. Mach. Intell.*, vol. 34, no. 11, pp. 2274–2282, Nov. 2012.

[19] L. Zhou, X. Yu, B. Li, C. Zheng, J. Liu, Q. Liu, and K. Guo, "Damping inter-area oscillations with large-scale PV plant by modified multiple-model adaptive control strategy," *IEEE Trans. Sustain. Energy*, vol. 8, no. 4, pp. 1629–1636, Oct. 2017.

[20] M. Ghofrani, M. de Rezende, R. Azimi, and M. Ghayekhloo, "K-means clustering with a new initialization approach for wind power forecasting," in *Proc. IEEE/PES Transmiss. Distrib. Conf. Expo. (TD)*, Dallas, TX, USA, May 2016, pp. 1–5.
[21] Y. Guo, H. Gao, and Q. Wu, "A combined reliability model of VSC-HVDC connected offshore wind farms considering wind speed correlation," *IEEE Trans. Sustain. Energy*, vol. 8, no. 4, pp. 1637–1646, Oct. 2017.
[22] R. Fang, R. Shang, M. Wu, C. Peng, and X. Guo, "Application of gray relational analysis to k-means clustering for dynamic equivalent modeling of wind farm," *Int. J. Hydrogen Energy*, vol. 42, pp. 20154–20163, Aug. 2017.
[23] E. T. Al-Shammari, S. Shamshirband, D. Petković, E. Zalnezhad, P. L. Yee, R. S. Taher, and Z. Cojbašić, "Comparative study of clustering methods for wake effect analysis in wind farm," *Energy*, vol. 95, pp. 573–579, Jan. 2016.
[24] S. C. Chen Wang, H. Shen, N. Gao, L. Zhu, and H. Lan, "Dynamic equivalence for wind farms based on clustering algorithm," *Proc. CSEE*, vol. 32, no. 4, pp. 11–18, 2012.
[25] G. Fan, K. Shi, T. Zheng, L. Feng, and Z. Li, "Cluster analysis of grid-connected large scale wind farms," *Power Syst. Technol.*, vol. 35, no. 11, pp. 62–66, 2011.
[26] J. Wang, M. Han, Z. Wang, S. Wei, and Y. Gu, "Lumping and electromechanical transient modeling of large-scale wind farm," in *Proc. Int. Conf. Power Syst. Technol. (POWERCON)*, Chengdu, China, Oct. 2014, pp. 2840–2845.
[27] J. Ouyang, Y. Diao, D. Zheng, C. Xiao, and X. Xiong, "A clustering method of coherent generators during electromagnetic transient process based on similar degrees of current trajectories for doubly fed wind farms," *Proc. CSEE*, vol. 37, no. 10, pp. 2896–2904, 2017.
[28] O. Jinxin, D. Yanbo, Z. Di, Y. Rui, Z. Xi, and X. Xiaofu, "Dynamic equivalent model of doubly fed wind farm during electromagnetic transient process," *IET Renew Power Gen.*, vol. 11, pp. 100–106, Jan. 2017.
[29] A. El-Naggar, and I. Erlich, "Analysis of fault current contribution of Doubly-Fed Induction Generator Wind Turbines during unbalanced grid faults," *Renew. Energy*, vol. 91, pp. 137–146, Jun. 2016.
[30] J. J. Justo, F. Mwasilu, and J.-W. Jung, "Doubly-fed induction generator based wind turbines: A comprehensive review of fault ride-through strategies," *Renew. Sustain. Energy Rev.*, vol. 45, pp. 447–467, May 2015.
[31] Y. Gao, R. Qu, D. Li, J. Li, and G. Zhou, "Design of a dual-stator LTS Vernier machine for direct-drive wind power generation," *IEEE Trans. Appl. Supercond.*, vol. 26, no. 4, Jun. 2016, Art. no. 5204505.
[32] A. Rodriguez and A. Laio, "Clustering by fast search and find of density peaks," *Science*, vol. 344, no. 6191, pp. 1492–1496, Jun. 2014.
[33] B. Wang, X. Wang, X. Wang, C. Shao, P. D. Judge, and T. C. Green, "An analytical approach to evaluate the reliability of offshore wind power plants considering environmental impact," *IEEE Trans. Sustain. Energy*, vol. 9, no. 1, pp. 249–261, Jan. 2018.
[34] Z. Mi, X. Su, Q. Yang, Y. Wang, and T. Wu, "Multi-machine representation method for dynamic equivalent model of wind farms," *Trans. China Electrotech. Soc.*, vol. 25, no. 5, pp. 162–169, 2010.
[35] A. Ramirez, A. Mehrizi-Sani, D. Hussein, M. Matar, M. Abdel-Rahman, J. Chavez, A. Davoudi, and S. Kamalasadan, "Application of balanced realizations for model-order reduction of dynamic power system equivalents," *IEEE Trans. Power Del.*, vol. 31, no. 5, pp. 2304–2312, Oct. 2016.
[36] L. M. Fernández, J. R. Saenz, and F. Jurado, "Dynamic models of wind farms with fixed speed wind turbines," *Renew. Energy*, vol. 31, no. 8, pp. 1201–1230, 2006.

MINGYANG LIU (S'18) received the B.S. degree in electrical engineering, in 2013. He is currently pursuing the Ph.D. degree in electrical engineering with Hohai University, Jiangsu, Nanjing, China. His main research interest includes wind power generation technology.

WENXIA PAN received the B.S. and M.S. degrees from Wuhan University, Wuhan, China, in 1982 and 1987, and the Ph.D. degree from Hohai University, Nanjing, China, in 2004, where she is currently a Professor of electrical engineering. She has published two research books. She has authored or coauthored over 100 journal papers. Her current research interests include renewable energy generation systems and high-voltage and insulation technology.

YIBO ZHANG received the M.S. degree from Hohai University, Nanjing, China, in 2018. She is currently an Assistant Engineer with State Grid Henan Electric Power Corporation Maintenance Company, Zhengzhou, China. Her main research interest includes wind power generation technology.

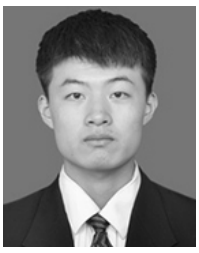

KUN ZHAO received the B.S. degree in electrical engineering, in 2017. He is currently pursuing the M.S. degree in electrical engineering with Hohai University, Nanjing, Jiangsu, China. His main research interests include wind power generation technology, and high voltage and insulation technology.

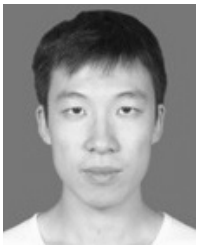

SHIDA ZHANG received the M.S. degree from Hohai University, Nanjing, China, in 2018. He is currently an Assistant Engineer with State Grid Henan Electric Power Corporation Maintenance Company, Zhengzhou, China. His main research interest includes the analysis and the optimization on power systems.

TONGCHUI LIU received the B.S. degree from Xuchang University, Xuchang, China, in 2012, and the M.S. degree from Hohai University, Nanjing, China, in 2015. He is currently pursuing the Ph.D. degree in electrical engineering with Hohai University, Nanjing, China. He is also an Engineer with State Grid Ningbo Power Supply Company, Ningbo, China. His main research interest includes renewable energy generation technology.